15th World Congress on Computational Mechanics (WCCM-XV)
8th Asian Pacific Congress on Computational Mechanics (APCOM-VIII)
Virtual Congress: 31 July – 5 August 2022
S. Koshizuka (Ed.)

SIMULATION OF BEARING CAPACITY OF PILE IN CRUSHABLE SOIL

TRONG-NGHIA NGUYEN[1,2], MAMORU KIKUMOTO[1], FLORINCE[1] AND RAHMAT KURNIAWAN[1]

[1] Department of Civil Engineering, Yokohama National University, Yokohama, Japan. 240-8501
[2] Faculty of Civil Engineering, Ho Chi Minh City Open University, Vietnam. 722700

E-mail. nghia.nt@ou.edu.vn,
kikumoto@ynu.ac.jp,
florince-tm@ynu.jp,
rahmat.kurniawan@si.itera.ac.id.

Key Words: Bearing capacity, Simulation, Crushable soil, Pile

Abstract: *Crushable soils such as volcanic soils, carbonate sand or decomposed granites whose grains are easily break under foundation pressure, especially, large magnitude of stresses under pile tips. When the grains are crushed, particle size distribution (PSD) varies followed by higher compressibility of these soils. Pile foundation's settlement in crushable soils tends to be increased. Nonetheless, design code for bearing capacity of pile in crushable soil is still unavailable leading to a lot of difficulties for engineers to have an appropriate foundation design. This paper introduces a constitutive model for soils which takes account of the breakage mechanics including the evolutions of PSD and the compressibility due to grain crushing. The model is implemented in a finite element code to simulate pile penetration in crushable soil. Finally, the particle breakage around pile's tip is examined.*

1 INTRODUCTION

Crushable soils are extensively studied due to their widely distributions around the world and their weak-grain structure reducing the resistance of foundation structures. Crushable soils include carbonate soils, volcanic soils and decomposed granite are distributed at the tropically coastal, high volcanic activity and high weathering regions, respectively. The fundamental behaviour of these soils is their weak grain can be easily crushed under the applied stress. As the grains crushed, particle size distribution (PSD) change following by the contraction of soil sample. Thus, higher deformation are detected for the foundation structures which are rested on the crushable soils. Senders, et al. [1], reported a reduction of pile's resistance when they were installed into the carbonate soil in the North-West coast of Australia. Furthermore, the end bearing resistance and skin resistance reduced due to particle crushing were presented by the physical models by [2]. The physical models by [2] and [3] also demonstrated the crushing zones around pile's tip and pile's shaft. Therefore, the pile's resistance is reduced when piles are rested on the crushable soil.

The above evidence raises questions on how to obtain a rational solution to examine the

response of pile foundation on the crushable soils. Classical foundation design methods such as [4-7] based on the equilibrium equations and assumptions of rigid-plastic mechanism which had not considered the particle crushing effect. Therefore, the current design codes based on these classical formulations lead to overestimate the pile's resistance on these crushable soils. Numerical methods considering the effect of particle crushing seem to be the appropriated method to determine the responses of pile on the crushable soils. Zhang, et al. [8], performed simulations on Eulerian finite framework based on a constitutive model considering breakage mechanics theory [9]. However, there are still several limitations in this simulation. Firstly, the constitutive model based on breakage mechanics theory [9] validated with only drained triaxial shear tests while it was not confirmed with any consolidation tests. As noticed by many researchers ([2, 3]), the stress zones under pile's tip and surrounding pile's shaft are various combinations of stress. Thus, the validations of the constitutive model with consolidation test and shear tests are necessary. Secondly, the initial vertical and horizontal stress distributed uniformly which cannot reflect the in-situ condition where linear distribution of vertical stress caused by the gravity force. Finally, the breakage responses around pile's tip when pile was displaced was not examined. It is benefit for engineers to understand the mechanical breakage at the pile's tip.

In this study, a constitutive model is proposed considering the effect of particle crushing through the evolution of PSD. The proposed model is validated with a wide range of experimental results such as: isotropic compression test; consolidated undrained triaxial test; consolidated drained triaxial test with constant mean effective stress; consolidated drained triaxial test with constant radial stress. Then, the constitutive model is implemented into FEM software (PLAXIS) to examine the pile's response. Initial stress state with the effect of gravitation has also been generated. The simulation results show that current analysis can capture the breakage phenomena around pile's tip and pile's shaft. Finally, the breakage around pile's tip is examined in this study.

2 CONSTITUTIVE MODEL

Identifying the critical state line (CSL) for sand is a crucial task to establish a constitutive model. Experimental evidence by Been and Jefferies [10] for Kogyuk 350 sand; [11] and [12] for Dogs Bay sand showed that the CSL had a linear shape in *e*-log*p'* plane. Thus a simple linear CSL ([13-15]) is employed here, in which, the critical specific volume , v_{cs} , can be expressed through the mean effective stress, p', as:

$$v_{cs} = \Gamma - \lambda \ln \frac{p'}{p_a} \tag{1}$$

where Γ is the specific volume on the critical state line when mean effective stress, p', is 98 kPa; p_a is the atmospheric pressure; λ is the compression index.

As noted by many researchers, the particle crushing caused downward parallel shift in the critical state line (CSL) in *e*-log*p'* space (Figure 1). Therefore, a new state parameter, ψ_c, representing the downward shift of CSL similar to the reduction of specific volume in the study of [16] is introduced:

$$v_{cs} = \Gamma - \lambda \ln \frac{p'}{p_a} - \psi_c \tag{2}$$

When particles are crushed, the PSD changes. In order to capture the variation of PSD, a simple grading index, I_G was presented by [17]. Based on experimental results by [18, 19], The grading index, I_G , depended on the applied stress. Thus, former function of grading index, I_G,

([16]) expressed through the crushing resistance pressure, p_x, is ultilized as:

$$I_G = 1 - \exp\left(\frac{p_x - p_{xo}}{p_r}\right)^n \tag{3}$$

where p_{xo} is the initial crushing stress; p_r is the crushing resistance; n is a material constant; the crushing stress , p_x , composed of mean effective stress , p', and deviator stress, q, is considered in [16] as $p_x = p'\left\{1+\left(\frac{q}{M_x p'}\right)^3\right\}$. Thus the crushing surface is:

$$f_x = p_x - p'\left\{1+\left(\frac{q}{M_x p'}\right)^3\right\} \tag{4}$$

Where M_x parameter controlling the shape of crushing surface. when the crushing happens, grading index, I_G, increases and the state parameter of ψ_c increases, correspondingly. Thus, in this study, a simple linear relationship between grading index, I_G, and the state parameter of ψ_c is proposed as:

$$\psi_c = \xi I_G \tag{5}$$

where ξ is the volumetric distance from the CSL with $I_G = 0.0$ to the CSL with $I_G = 1.0$ (Figure 1). In this study, the state parameter, ψ_s, for sand proposed by [10] (as the specific volumn distance from the current specific state, v , to the specific volume of critical state , v_{cs} , at the same mean effective stress, p') is considered as (Figure 1):

$$\psi_s = v - v_{cs} \tag{6}$$

The state parameter , ψ_s, indicated the dilation or contraction tendency of sand when it is sheared ([10]). Thus, the strength of soil may have a certain relationship with this state parameter. In the Severnt Trent sand model propopsed by [15], the available strength, η_u, was defined as a function depending on the state parameter, ψ_s as:

$$\eta \le \eta_u(\psi_s) \tag{7}$$

Considering the simple assumption that the available strength is a nonlinear function which can express through the state parameter, ψ_s, as:

$$\eta_u(\psi_s) = M\sqrt{2^{1-k\psi_s} - 1} \tag{8}$$

Where k is a positive constitutive parameter

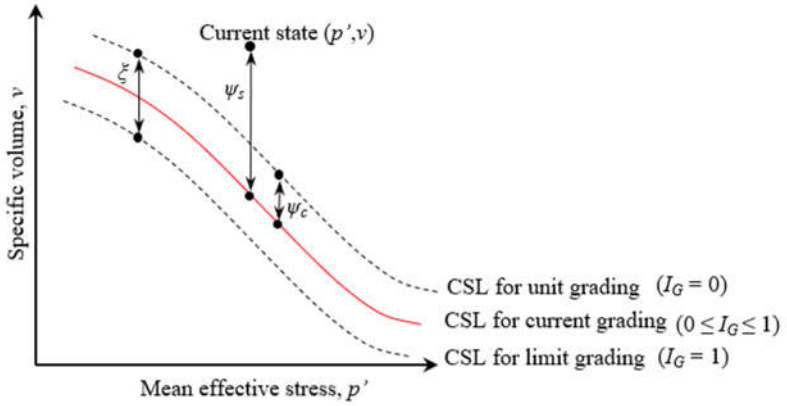

Figure 1: Critical state line in p'– v plane for the crushable soils

Substituting Eqs. (2), (6), (8) into Eq.(7) , an upper threshold of specified volume can be

obtained as:

$$v \le v_u = -\lambda \ln \frac{p'}{p_a} + \frac{1}{k}\left[1 - \frac{\ln\left\{1+\left(\frac{\eta}{M}\right)^2\right\}}{\ln 2}\right] + \Gamma - \psi_c \tag{9}$$

Eq. (9) is also play a role as the state boundary surface (SBS) for sand. Where the soil's state never exceeds beyond the SBS, thus the bounding surface , $\tilde{f}$, can be derived as:

$$\tilde{f} = v - v_u \le 0 \tag{10}$$

In the classical critical state model, the soil's state below the bounding surface is decribed as the purely elastic behavior whereas the actual behavior is elastoplastic irrevesible at this state. Thus, in order to describe a smooth transition between these states, a state parameter of volumetric distance , Ω, from current specific volumn to the specific volumn on SBS is presented to scale the current state to the normal bounding surface:

$$\Omega = v_u - v \tag{11}$$

Based on the Eq. (10) and (11), the yield surface function can be obtained as:

$$f = v - v_u + \Omega \equiv 0 \tag{12}$$

Here, the yield function is identically equal to zero.

The variables $\left(v, p', \eta, \varepsilon_v^p, \Omega, \psi_c\right)$ are hereafter denoted as $\left(v_o, p'_o, \eta_o, \varepsilon_{vo}^p (=0), \Omega_o, \psi_{co}\right)$ at initial state and $\left(v, p', \eta, \varepsilon_v^p, \Omega, \psi_c\right)$ at the current state. By substituting Eq.(9) into (12); appling the initial state of $f\left(v_o, p'_o, \eta_o, \varepsilon_{vo}^p, \Omega_o, \psi_{co}\right) \equiv 0$; and using assumption of associtate flow rule at the critical state $\left.\frac{\partial f}{\partial p'}\right|_{\eta=M} = 0$, the yield surface function can be finally obtained as:

$$f\left(v, p', \eta, \varepsilon_v^p, \Omega, \psi_c\right) = (\lambda - \kappa) \ln \frac{p'\left\{1+\left(\frac{\eta}{M}\right)^2\right\}}{p'_o\left\{1+\left(\frac{\eta_o}{M}\right)^2\right\}} + (\Omega - \Omega_o) + (\psi_c - \psi_{co}) - v_o \varepsilon_v^p \tag{13}$$

where the first term in the right hand side of the equation is related to the stress state and the remaining terms on the right hand side of the equation are related to the hardening parameters. The consistancy condition is:

$$\dot{f} = \frac{\partial f}{\partial \boldsymbol{\sigma}'} \dot{\boldsymbol{\sigma}}' + \frac{\partial f}{\partial \varepsilon_v^p} \dot{\varepsilon}_v^p + \frac{\partial f}{\partial \Omega} \dot{\Omega} + \frac{\partial f}{\partial \psi_c} \dot{\psi}_c \equiv 0 \tag{14}$$

Hardening rule for plastic volumetric strain with assumption of associated flow rule:

$$\frac{\partial f}{\partial \varepsilon_v^p} \dot{\varepsilon}_v^p = -v_o \dot{\Lambda} tr \frac{\partial f}{\partial \boldsymbol{\sigma}'} \tag{15}$$

Hardening rule for the state parameter of volumetric distance, Ω, should decrease with the evolution of plastic deformation and converge to zero. Thus, a simple evolution rule for Ω is proposed as:

$$\frac{\partial f}{\partial \Omega} \dot{\Omega} = -\omega \Omega |\Omega| \left\| \dot{\varepsilon}^p \right\| \tag{16}$$

Where ω is a state parameter that controls the rate of evolution of Ω ,and $\left\| \dot{\varepsilon}^p \right\|$ is the norm of

the plastic strain rate.

Hardening rule for the state parameter relating to the crushing, ψ_c, is deduced from the evolution rule of grading index, I_G. From Eqs. (3) and (4) evolution rule of I_G can be determined as:

$$\dot{I}_G = \frac{\partial I_G}{\partial p_x}\dot{p}_x = \left(1 - I_G\right)\frac{\partial f_x}{\partial \boldsymbol{\sigma}'}\boldsymbol{\sigma}' \tag{17}$$

Thus, the hardening rule for ψ_c can be obtained through Eqs. (5) and (17) as:

$$\frac{\partial f}{\partial \psi_c}\dot{\psi}_c = \xi \dot{I}_G = \xi\left(1 - I_G\right)\frac{\partial f_x}{\partial \boldsymbol{\sigma}'}\boldsymbol{\sigma}' \tag{18}$$

Based on these hardening rules and stress-strain relationships in continuum mechanics, the plastic multiplier $\dot{\Lambda}$ and elastoplastic stress-strain relationship can be determined for the constitutive model.

3 VALIDATIONS OF THE CONSTITUTIVE MODEL

Table 1: Material's parameters for Dogs Bay sand

Parameters	Descriptions	Values
λ	compression index	0.150
κ	swelling index	0.015
Γ	specific volume on CSL at p' = 98 kPa	3.0
M	critical state stress ratio	1.65
ν_e	Poisson's ratio	0.2
ω	parameter for the rate of Ω	50
p_r	crushing resistance stress (kPa)	7500
M_x	parameter controlling the shape of crushing surface	0.95
ξ	volumetric distance between SBSs of I_G = 0 and I_G = 1	1.25
p_{xo}	initial crushing stress (kPa)	100
n	parameter for the ratio of crushing stress	1.55

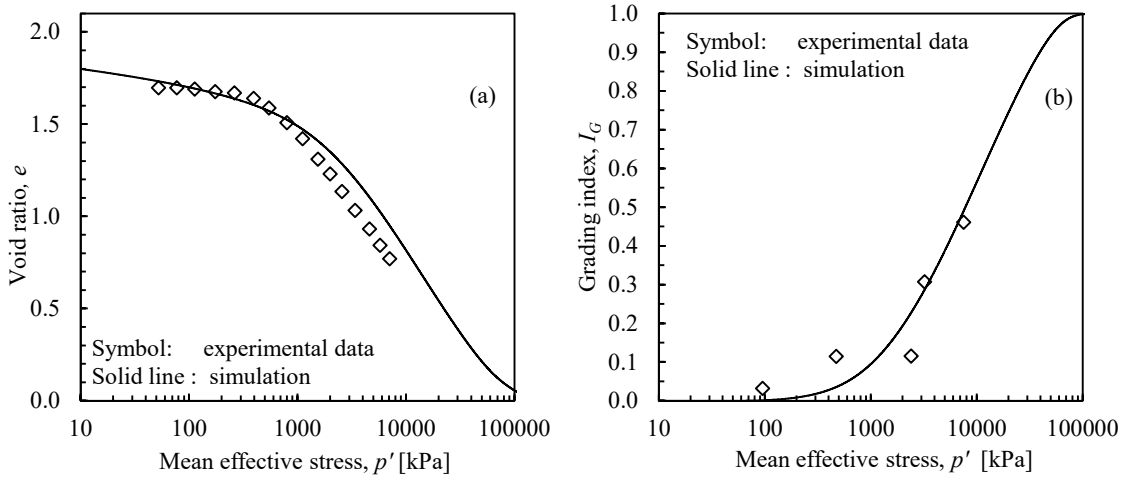

Figure 2: Comparison between simulation results by the proposed model and the experimental results in isotropic consolidation test: (a) Compression curves; (b) Grading index versus mean effective stress.

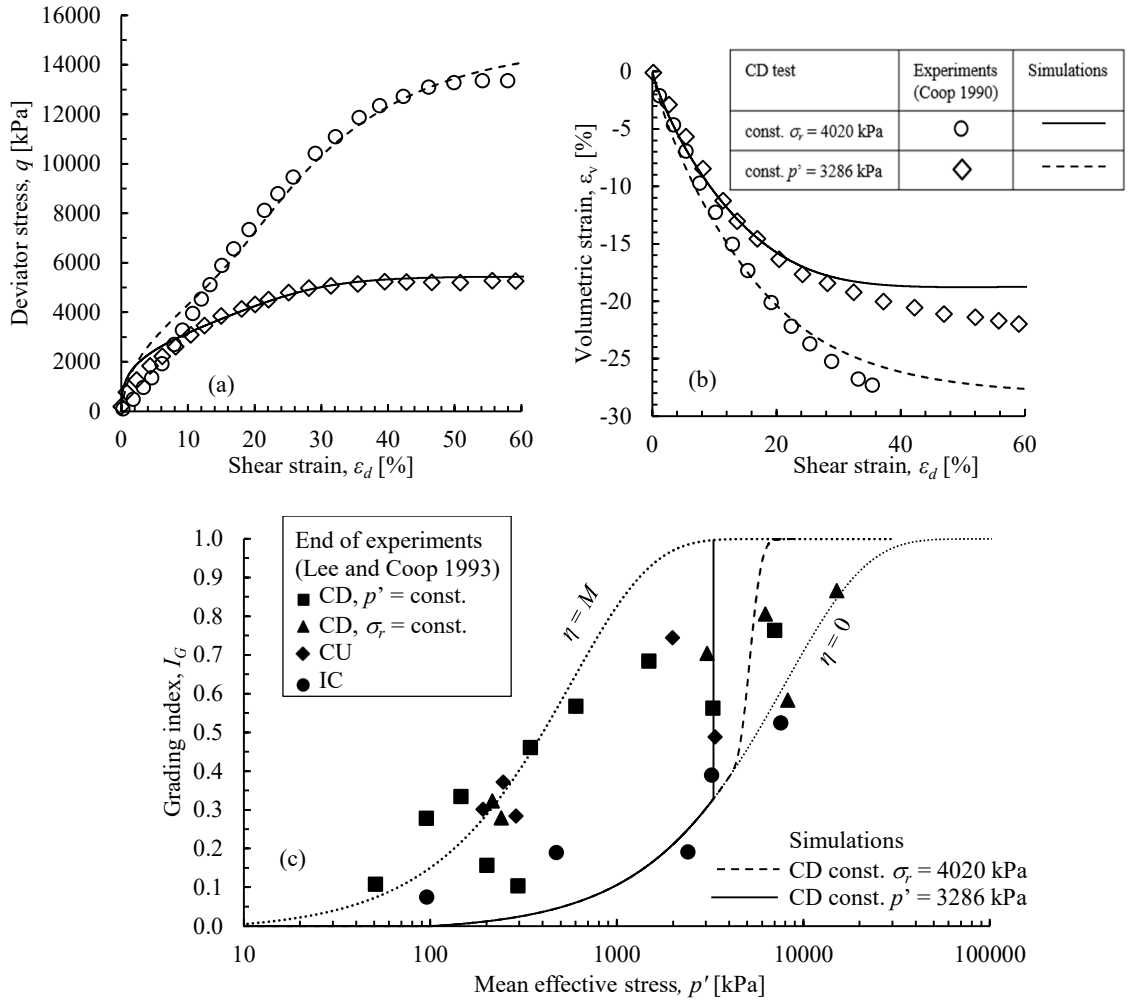

Figure 3: Comparison between simulation results by the proposed model and the experimental results in consolidated drained triaxial tests: (a) Deviator stress versus shear strain; (b) Volumetric strain versus shear strain; (c) Grading index versus mean effective stress.

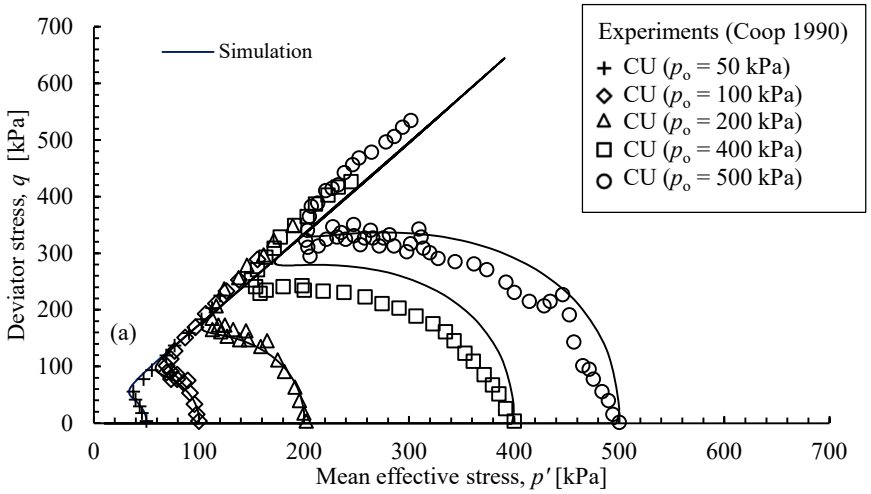

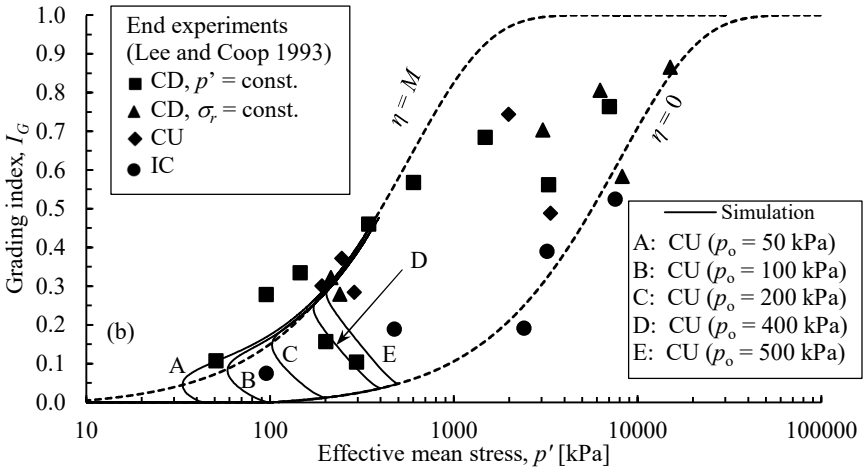

Figure 4: Comparison between simulation results by the proposed model and the experimental results in consolidated undrained triaxial tests: (a) Deviator stress versus mean effective stress; (b) Grading index versus mean effective stress.

The material parameters of Dogs Bay sand for the proposed model given in table 1 are used to validate with extensive tests of isotropic consolidation test (IC), consolidated drained triaxial tests (CD), and consolidated undrained triaxial tests (CU). Firstly, Coop and Lee [20], performed isotropic consolidation tests (IC) for Dogs Bay sand with the variation of grading indices shown in Figure 2. When the compressive stress increased, the grading index was also increased. The simulation results by the proposed model can capture the variations of stress-strain and grading index.

At high confining pressure, performance of the proposed model is validated by CD tests with constant mean effective stress ($p' = 3286$ kPa) and constant radial stress ($\sigma_r = 4020$ kPa) (Figures 3(a), 3(b), and 3(c)). Experimental results of the stress-strain and dilatancy's trend illustrated in Figures 3(a) and 3(b) are very well capture by the simulation results. Next, in the Figure 3(c), the grading index variation during IC and shearing state at high confining pressure show similar trend with the experimental results at the end of tests by [20].

Coop [12], performed a series of CU tests on Dogs Bay sand with different confining pressures from 50 kPa to 500 kPa shown in Figure 4(a). In this figure, the stress paths of CU tests are well predicted by the proposed model. Furthermore, the evolution of grading indices simulated by the proposed model also vary within the experimental ranges illustrated in Figure 4(b). These comparisons have confirmed the validity of the proposed model in capturing the stress-strain relationship and variations of grading index for the crushable soils.

4 SIMULATIONS OF PILE'S RESPONSE ON CRUSHABLE SOIL

The constitutive model is incorporated into FEM (PLAXIS) to examine the responses of pile on Dogs Bay sand when subjected to axial loading. Pile's diameter (D) is 1.0 m and pile length are 10m. Assuming the construction technique is replacement technique then the interface layer is assumed have the same strength parameters as Dogs Bay sand. Axial displacement is assigned at the pile head with gradually increase to the maximum value of $0.1D = 0.1$m. Initial condition is generated with gravity load with the initial soil state ($e_o = 1.7$, $I_G = 0.0$, $\gamma' = 17$ kN/m^3). Pile model is simply assumed as linear elastic model ($E = 27GPa, \nu = 0.2$). The model parameters for Dogs Bay sand are given in table 1.

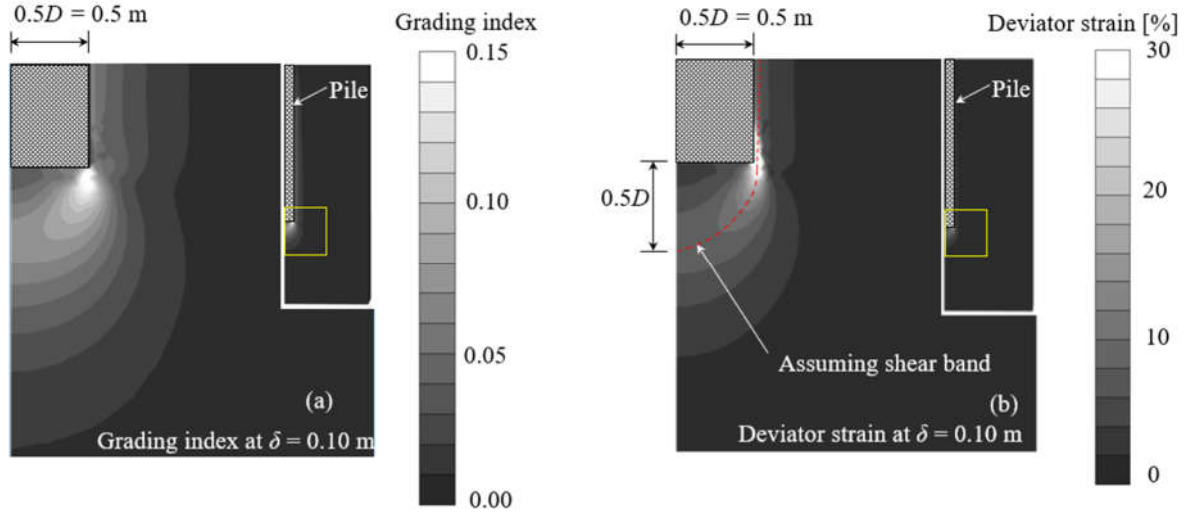

Figure 5: (a) Grading index distribution; (b) deviator strain distribution

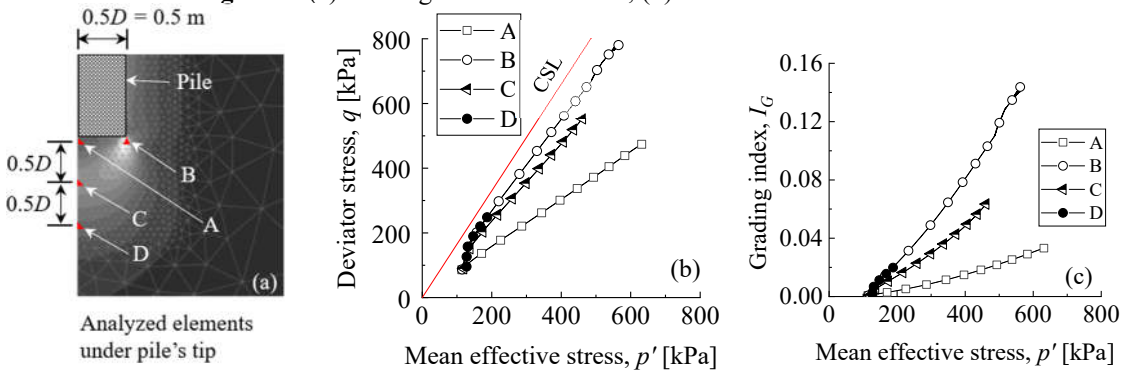

Figure 6: (a) analyzed elements under pile's tip; (b) stress paths of different locations; (c) variations of grading index of different locations

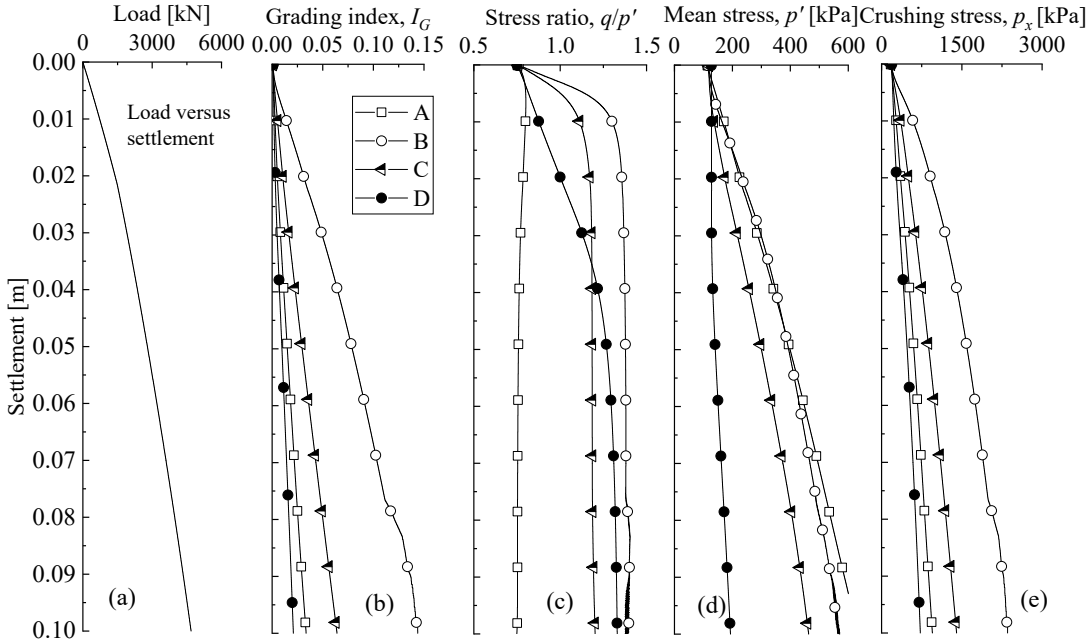

Figure 7: (a) Load settlement curve; (b) variations of grading indices with settlements; (c) variations of stress ratio with settlements; (d) variation of mean effective stress with settlements; (e) variations of void ratio with settlements.

Figure 5a shows the simulation results of grading index by the proposed model with high magnitude around pile's shaft and pile's tip. The crushing zone is approximately one pile's radius from the pile's shaft and two pile's diameter from pile's tip, in agreement with experimental results by [2]. Based on simulation results of deviator strain (Figure 5b), the failure model of pile on sand can be the punching shear model due to more concentration of deviator strain look like a cone shape beneath the pile. Thus, a simple assumption of shear band is proposed with starting along pile's shaft and extending one radius beneath pile's tip (Figure 5b). Based on the assumption of shear band, the load transferring mechanics of pile to surrounding soil is revealed, in which the axial load of pile is carried through the mobilized shearing stress along the shear band. The higher shearing stress along the shear band can cause more particle breakage which in turn reducing the pile's resistance.

The simulation results also reveal that the crushing zone beneath the pile distributed non-uniformly, especially more crushing concentrating at the pile's corner and along the assuming shear-band's zone. It is expected to examine the non-uniform distribution of crushing beneath the pile to understand the breakage responses when pile penetrating the crushing soils. For that purpose, four soil's elements beneath the pile's tip are selected (Figure 6a) where the elements B and C are on the assuming shear band zone; and elements A and D are outside the zone. The stress paths and variations of grading indices of these elements are shown in Figures 6b and 6c. As can be observed from the figures, elements B and C show higher deviator stress than elements A and D may come from their positions on the assuming shear band. However, the effective mean stress of element A is highest among these results (effective mean stress of element A > B > C > D) because element A locates right beneath the pile's center. In general, the soil's particles can be crushed under compression and shear forces, but they are more likely to break under shear forces than compression forces. The proposed model considers the stress state (p', q) or (η, p') inducing particle crushing (Eqs.3 and 4) and the model was also validated with both consolidation and shearing tests. The simulation results of elements B and C with higher grading indices than elements A and D (Figure 6c) reflect the reasonable breakage mechanics of the crushable soil in which more particle crushing occur at the assuming shear band than the outside zone.

Variations of stress ratio, grading index, mean effective stress and crushing stress of the four elements (A, B, C and D) with the settlement are illustrated in Figure 7 together with the load settlement curve. Element B at the pile corner show almost highest values of grading index, stress ratio, and mean effective stress and crushing stress, following by the element C with a similar trend. The stress ratio of element D (Figure 7c) increases gradually with the settlement due to larger distance from the pile's tip as compared to other elements indicating that the zone outside the assuming shear band also exhibiting an increase of deviator stress but lower value and slower transferring. Outside the assuming shear band zone (elements A and D), element A has high mean effective stress (Figure 7d) but low stress ratio (Figure 7c), meanwhile, element D has high stress ratio (Figure 7c) but low mean effective stress (Figure 7d). The proposed model determined the particle crushing based on combination of stress state (η, p') through the crushing stress, p_x . Thus, the stress state of element A (high mean effective stress and low stress ratio) and element B (low mean effective stress and high stress ratio) can lead to an approximate value of p_x and I_G .

5 CONCLUSIONS

In this study, the pile's response on crushable soils is studied through numerical simulation with the proposed constitutive model. The proposed constitutive model considering crushing effect through the downward shift of critical state line. A state boundary condition for sand is also established based on previous research of state parameter for sand and available strength

from the Servant Trent sand model. The model validation is carried out with series of tests from IC to CD and CU tests. Then, numerical simulation of pile on Dogs bays sand is examined. The results of simulation show particle crushing around pile's shaft and pile's tip which are agreement with experimental observation by previous researcher. Several findings can be summarized here:

The simulation results of deviator strain show that the failure model of pile can be the punching shear model with simple assuming shear band staring from the pile's shaft and extending one pile's radius beneath the pile's tip. The assumption of shear band zone can help to explain the load transfer mechanics of pile, in which, the axial load of pile is carried through the mobilized shear stress along the shear band.

Crushing profile surrounding the pile's tip is non-uniform due to the stress states of these soil's elements. The elements along the assuming shear band show higher grading indices due to higher deviator stress and mean effective stress inducing higher crushing stress. While the other elements locate outside the shear band experiences lower crushing stress leading to lower grading indices. The crushing happen along the assuming shear band may cause reduction of mobilized shear stress leading to reduction of pile resistance.

REFERNCES

[1] Senders, M. Banimahd, M. Zhang, T. and Lane, A. J. A. G. J. Piled foundations on the northwest shelf. *Australian Geomechanics Journal* (2013) **48**:149-160.

[2] Kuwajima, K. Hyodo, M. and Hyde, A. F. Pile Bearing Capacity Factors and Soil Crushabity. *Journal of Geotechnical and Geoenvironmental Engineering* (2009) **135**(7): 901-913.

[3] Yasufuku, N. and Hyde, A. F. L. Pile end-bearing capacity in crushable sands. *Géotechnique* (1995) **45**(4): 663-676.

[4] Prandtl, L. Hauptaufsätze: Über die Eindringungsfestigkeit (Härte) plastischer Baustoffe und die Festigkeit von Schneiden. *ZAMM - Journal of Applied Mathematics and Mechanics / Zeitschrift für Angewandte Mathematik und Mechanik* (1921) 1(1):15-20.

[5] Terzaghi, K. *Theoretical soil mechanics*. New York, NY, USA: Wiley, 1943.

[6] Vesić, A. S. Analysis of Ultimate Loads of Shallow Foundations. *Journal of the Soil Mechanics and Foundations Division* (1973) **99**(1): 45-73, 1973.

[7] Meyerhof, G. G. Some Recent Research on the Bearing Capacity of Foundations. *Canadian Geotechnical Journal*, (1963) **1**(1): 16-26.

[8] Zhang, C. Nguyen, G. D. and Einav, I. The end-bearing capacity of piles penetrating into crushable soils. *Géotechnique* (2013) **63**(5): 341-354.

[9] Einav, I. Breakage mechanics—Part I: Theory. *Journal of the Mechanics and Physics of Solids* (2007) **55**(6): 1274-1297.

[10] Been, K. and Jefferies, M. G. A state parameter for sands. *Géotechnique* (1985) **35**(2): 99-112.

[11] Bandini, V. and Coop, M. R. The Influence of Particle Breakage on the Location of the Critical State Line of Sands. *Soils and Foundations* (2011) 51(4): 591-600.

[12] Coop, M. R. The mechanics of uncemented carbonate sands. *Géotechnique* (1990) 40(4): 607-626.

[13] Wood, D. M. and Belkheir, K. Strain softening and state parameter for sand modelling. *Géotechnique* (1994) **44**(2): 335-339.

[14] Gajo, A. and Muir Wood, D. Severn–Trent sand: a kinematic-hardening constitutive model: the q–p formulation. *Géotechnique* (1999) **49**(5): 595-614.

[15] Gajo, A. and Muir Wood, D. A kinematic hardening constitutive model for sands: the

multiaxial formulation. *International Journal for Numerical and Analytical Methods in Geomechanics* (1999) **23**(9): 925-965.

[16] Kikumoto, M. Wood, D.M. and Russell, A. Particle Crushing and Deformation Behaviour. *Soils and Foundations*. **50**(4): 547-563.

[17] Muir Wood, D. The magic of sands— The 20th Bjerrum Lecture presented in Oslo, 25 November 2005. *Canadian Geotechnical Journal* (2007) **44**(11): 1329-1350.

[18] Lade, P. V. Yamamuro, J. A. and Bopp, P. A. Significance of Particle Crushing in Granular Materials. *Journal of Geotechnical Engineering*, (1996) **122**(4): 309-316

[19] Hardin, B. O. Crushing of Soil Particles. *Journal of Geotechnical Engineering*. (1985) 111(10): 1177-1192.

[20] Coop, M. and Lee, I. The behaviour of granular soils at elevated stresses. *in Predictive soil mechanics: Proceedings of the Wroth Memorial Symposium held at St Catherine's College, Oxford*, (1992) :27-29.